

Trapping of H_2^- in aluminum hydride, $\text{Al}_4\text{H}_{14}^-$

Cite as: J. Chem. Phys. **155**, 121101 (2021); <https://doi.org/10.1063/5.0066449>

Submitted: 10 August 2021 . Accepted: 12 September 2021 . Published Online: 29 September 2021

Boggavarapu Kiran,  Kit H. Bowen and  Anil K. Kandalam



View Online



Export Citation



CrossMark

ARTICLES YOU MAY BE INTERESTED IN

[The electron affinity of the uranium atom](#)

The Journal of Chemical Physics **154**, 224307 (2021); <https://doi.org/10.1063/5.0046315>

[The superatomic state beyond conventional magic numbers: Ligated metal chalcogenide superatoms](#)

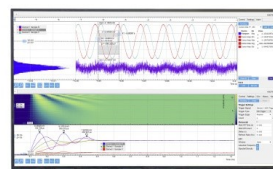
The Journal of Chemical Physics **155**, 120901 (2021); <https://doi.org/10.1063/5.0062582>

[How accurate are EOM-CC4 vertical excitation energies?](#)

The Journal of Chemical Physics **154**, 221103 (2021); <https://doi.org/10.1063/5.0055994>

Challenge us.

What are your needs for
periodic signal detection?



Zurich
Instruments

Trapping of H_2^- in aluminum hydride, $\text{Al}_4\text{H}_{14}^-$

Cite as: J. Chem. Phys. 155, 121101 (2021); doi: 10.1063/5.0066449

Submitted: 10 August 2021 • Accepted: 12 September 2021 •

Published Online: 29 September 2021



View Online



Export Citation



CrossMark

Boggavarapu Kiran,^{1,a)} Kit H. Bowen,²  and Anil K. Kandalam^{3,a)} 

AFFILIATIONS

¹ Department of Chemistry and Physics, McNeese State University, Lake Charles, Louisiana 70609, USA

² Departments of Chemistry and Materials Science, Johns Hopkins University, Baltimore, Maryland 21218, USA

³ Department of Physics and Engineering, West Chester University of PA, West Chester, Pennsylvania 19341, USA

^{a)} Authors to whom correspondence should be addressed: kiran@mcneese.edu and akandalam@wcupa.edu

ABSTRACT

Ever since our first experimental and computational identification of Al_4H_6 as a boron analog [X. Li *et al.*, *Science* **315**, 356 (2007)], studies on aluminum hydrides unveiled a richer pattern of structural motifs. These include aluminum-rich hydrides, which follow shell closing electron counting models; stoichiometric clusters (called *baby crystals*), which structurally correspond to the bulk alane; and more. In this regard, a mass spectral identification of unusually high intense peak of $\text{Al}_4\text{H}_{14}^-$, which has two hydrogen atoms beyond stoichiometry, has remained mostly unresolved [X. Li *et al.*, *J. Chem. Phys.* **132**, 241103 (2010)]. In this Communication, with the help of global minima methods and density functional theory-based calculations, we identify the lowest energy *bound* structure with a unique Al–H–H–Al bonding. Our electronic structural analysis reveals that two Al_2H_6 units trap a transient, metastable H_2^- . In other words, three stable molecules, two Al_2H_6 and an H_2 , are held together by a single electron. Our studies provide a pathway to stabilize transient species by making them part of a more extensive system.

Published under an exclusive license by AIP Publishing. <https://doi.org/10.1063/5.0066449>

Hydrogen anion (H_2^-), the simplest of all molecular anions, is considered to play an important role in several collision processes, which is, however, metastable with a short lifetime. Despite being very transient in nature, several ingenious experiments had been devised to verify the existence of the molecule. After several attempts by various groups, Gosler *et al.* provided the first unambiguous experimental evidence¹ of rotationally excited H_2^- and D_2^- . Recently, Rudnev *et al.* provided the first photo-detachment spectrum² of H_2^- , further cementing the evidence on the existence of H_2^- . Note that the hydrogen molecule has negative electron affinity (−1.03 eV), which implies that the addition of an electron to the ground state of H_2 is endothermic. This is understandable as the additional electron occupies the anti-bonding orbital, and it explains the elusive nature.

One way to stabilize H_2^- is to reduce the destabilizing nature of the anti-bonding orbital. This can be accomplished by making the anion a part of a larger molecular system. Aluminum hydrides provide such an opportunity. Over the last decade or so, we have identified several aluminum hydrides (Al_nH_m), including aluminum rich hydrides ($n > m$) (jellium clusters),^{3,4} analogs of boron hydrides⁵ ($n \sim m$), and stoichiometric clusters ($m = 3n$), which form *baby crystals*.⁶ In addition, we have shown⁷ that negatively charged aluminum hydrides can expand beyond stoichiometric Al_nH_{3n} by

taking additional hydrogen atoms ($\text{Al}_n\text{H}_{3n+1}$) to form long chain-like structures and cyclic ring structures. It was identified that the ion intensities for $\text{Al}_n\text{H}_{3n+1}$ species were significantly stronger than the ion intensities of Al_nH_{3n} , suggesting enhanced stabilities of $\text{Al}_n\text{H}_{3n+1}$ species. Interestingly, a new species, $\text{Al}_4\text{H}_{14}^-$, which has one extra hydrogen than the expected $\text{Al}_n\text{H}_{3n+1}$, was also observed in these experiments.⁷ More strikingly, in the mass spectrum, the ion intensity of $\text{Al}_4\text{H}_{14}^-$ was double that of $\text{Al}_4\text{H}_{13}^-$, thus indicating an unusually (thermodynamically) stable $\text{Al}_4\text{H}_{14}^-$. Despite these interesting features and the geometrical structure, a satisfactory explanation for the high intense mass peak of $\text{Al}_4\text{H}_{14}^-$ has remained largely unresolved. In this Communication, we will show that the lowest energy *bound* isomer of $\text{Al}_4\text{H}_{14}^-$ is where the H_2^- is trapped between two Al_2H_6 units. This unprecedented arrangement ushers in a new bonding scheme.

We have employed an unbiased systematic structure search based on the genetic algorithm (GA) method⁸ as implemented in TURBOMOLE⁹ along with several other isomers based on our past knowledge of aluminum hydride clusters to identify the lowest and other higher energy isomers of $\text{Al}_4\text{H}_{14}^-$ species. Both the initial population and the subsequent generations were fully optimized with the BP/def2-SV(p) level of theory. The validity of this approach was tested and established in our earlier work on aluminum hydride

clusters.⁶ The lowest energy and several other higher energy isomers from the GA were reoptimized using the Gaussian09 program suite.¹⁰ In this step, the B3LYP functional form,^{11,12} along with the augmented CC-pVTZ basis set, was employed. We have also carried out coupled-cluster single double triple [CCSD(T)] calculations with the CC-pVTZ basis set on B3LYP/aug-CC-pVTZ optimized geometries to determine the relative energies between various low energy isomers. In addition, we have carried out potential energy scan of the lowest energy structure at different H–H distances at both B3LYP and CCSD(T) levels using the CC-pVDZ basis set. Vibrational frequency calculations were done for all the reported isomers, and they are found to be minima on the potential energy surface.

Our calculations resulted in two classes of isomers: (1) structures in which $\text{Al}_4\text{H}_{14}^-$ exists as a *complex*, such as an $\text{Al}_4\text{H}_{12}^-$ moiety weakly interacting with H_2 , and (2) *bound* structures, wherein every atom is chemically bonded to another atom in the cluster. Among these two classes of isomers, the *complex(or an adduct)*-like structures can be ruled out based on two reasons. First, it is worth reminding here that among the reported⁷ mass peaks of Al_4H_m^- ($m = 12, 13, \text{ and } 14$), the ion intensity corresponding to $\text{Al}_4\text{H}_{14}^-$ was the strongest, indicating an enhanced stability of $\text{Al}_4\text{H}_{14}^-$. Such a high intensity in the mass spectrum indicates that the experimentally observed $\text{Al}_4\text{H}_{14}^-$ is highly unlikely to have a *complex*-like structure, wherein an $\text{Al}_4\text{H}_{12}^-$ moiety weakly interacts with

H_2 . Next, the *neutral* Al_4H_{12} is a highly stable cluster. It is well known that if a neutral cluster of a specific size is highly stable, then its anionic counterpart does not usually result in a high intense mass peak. So, it is again unlikely that the high intense peak of $\text{Al}_4\text{H}_{14}^-$ is a result of complex-like structures containing $\text{Al}_4\text{H}_{12}^-$. We, thus, conclude that only the *bound* structures (in which all the atoms were bonded to each other in one way or the other) are responsible for the experimentally observed $\text{Al}_4\text{H}_{14}^-$. So, rest of our discussion is focused only on the *bound* structures of $\text{Al}_4\text{H}_{14}^-$ obtained from our GA and density functional theory (DFT)-based calculations.

Figure 1 displays the most stable *bound* structures that we have identified in our calculations. They reveal several polymer-like chain structures in which the aluminum atoms have either fourfold or fivefold coordination. However, unlike in the case of $\text{Al}_n\text{H}_{3n+1}^-$ species,⁷ the *cyclic* (ring-like) bound structures were found to be very high in energy ($\Delta E \geq 0.4 \text{ eV}$) for $\text{Al}_4\text{H}_{14}^-$. The lowest energy isomer, structure **1a**, can be considered as two Al_2H_6 units connected by an H_2^- unit. The next higher energy isomer, structure **1b**, is reminiscent of our previously reported⁷ lowest energy chain-like structure of $\text{Al}_4\text{H}_{13}^-$, with the additional hydrogen atom bound to one of the terminal aluminum atoms, resulting in a fivefold coordination for that terminal metal atom. This structure can be considered as a combination of Al_2H_7 and Al_2H_7^- units. It is to be noted here that structure **1b** was reported as the lowest energy

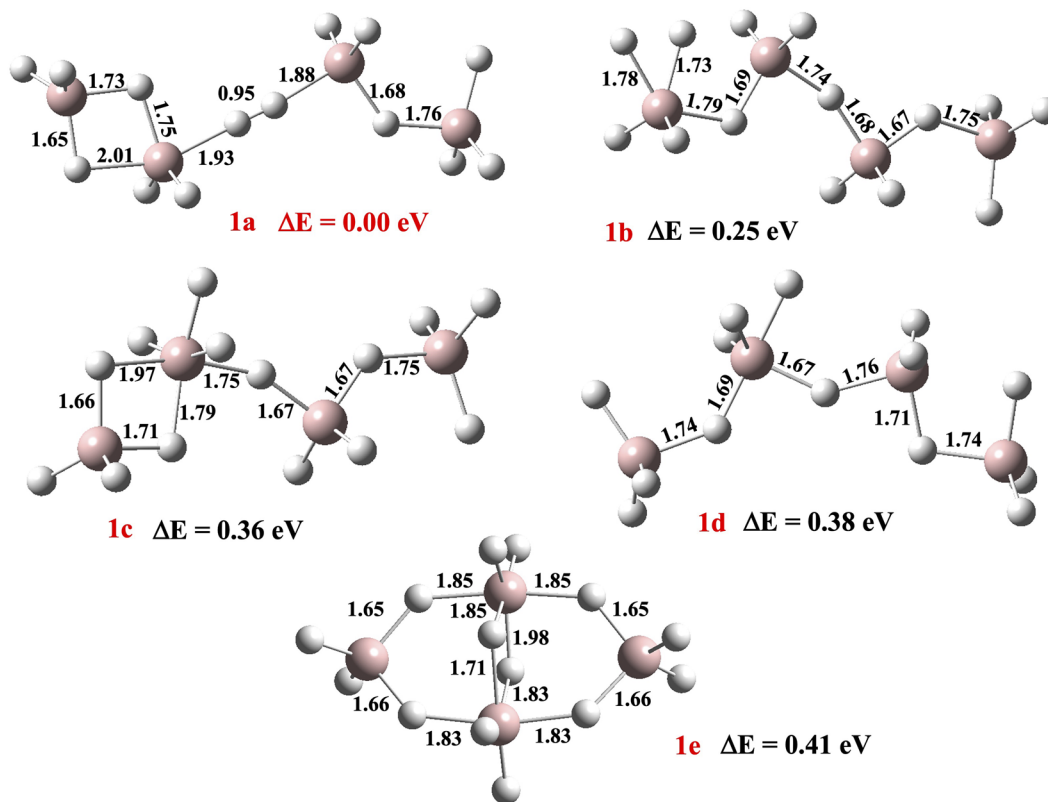


FIG. 1. The lowest energy bound isomers of $\text{Al}_4\text{H}_{14}^-$ and their relative energies. Also shown are the selected bond lengths.

isomer in an earlier computational study.¹³ In that study, the structure and stability of $\text{Al}_4\text{H}_{14}^-$ were studied at B3LYP/aug-cc-pVTZ and CCSD(T)/aug-cc-pVTZ levels. To have a fair comparison between our results and the previously reported results,¹³ we have carried out CCSD(T) energy calculations on the B3LYP optimized structures. Our reported structure **1a** was found to be lower in energy than the previously reported isomer (structure **1b**) at the CCSD(T) level of calculation as well, thereby confirming the energy ordering obtained at the B3LYP level of calculations. Thus, the relative energies in Fig. 1 and in the discussion of the remainder of this work are all calculated at the B3LYP/aug-cc-pVTZ level, unless otherwise stated. It is noteworthy here that even though the stabilization of H_2^- using molecular traps, such as between two LiCN molecules,¹⁴ has been reported in the past, as to our knowledge, this is the first time trapping of H_2^- is reported using aluminum hydrides. Structures **1a** and **1b** are followed by two more chain-like structures, **1c** and **1d** (see Fig. 1). Isomer **1c** can also be seen as a combination of Al_2H_7 and Al_2H_7^- units. However, unlike in the case of isomer **1b**, in the case of isomer **1c**, neither of the terminal aluminum atoms have a fivefold coordination, but an inner aluminum atom has a sixfold coordination. Finally, there is a cyclic (ring-like) structure, isomer **1e**, in which two non-adjacent aluminum atoms are bridged by two hydrogen atoms. This structure can be seen as an extension of the double-ring polymeric structure of $\text{Al}_4\text{H}_{13}^-$, reported in our previous study,⁷ with the additional hydrogen atom forming another bridge between the same set of non-adjacent aluminum atoms. Thus, in this isomer, the two di-hydrogen bridged aluminum atoms exhibit hexa-coordination. This ring-like isomer with two hexa-coordinated aluminum atoms (isomer **1e**) can also be considered as a part of the ground state structure of Al_6H_{18} (*baby crystal*), reported previously.⁶

The NPA charge analysis of structure **1a** revealed that there exist three distinct units making up the lowest energy bound structure of $\text{Al}_4\text{H}_{14}^-$: the left-side Al_2H_6 unit with a charge of $-0.3e$, the H_2 unit in the middle with a charge of $-0.28e$, and the Al_2H_6 unit on the right side with a charge of $-0.42e$. The stability of structure **1a** against dissociation into smaller aluminum-hydride units was studied by calculating the fragmentation energies along two different pathways using the following

equations:

Fragmentation into Al_2H_7 and Al_2H_7^- units :

$$E_1 = [E(\text{Al}_4\text{H}_{14}^-) - E(\text{Al}_2\text{H}_7^-) - E(\text{Al}_2\text{H}_7)],$$

Fragmentation into Al_2H_6 , Al_2H_6^- , and H_2 :

$$E_2 = [E(\text{Al}_4\text{H}_{14}^-) - E(\text{Al}_2\text{H}_6^-) - E(\text{Al}_2\text{H}_6) - E(\text{H}_2)].$$

These fragmentation pathways are all found to be exothermic, with the calculated fragmentation energies of $E_1 = -1.11$ eV and $E_2 = -0.37$ eV. Fragmentation into $\text{Al}_4\text{H}_{12}^-$ and H_2 units and fragmentation into $\text{Al}_4\text{H}_{13}^-$ and H are not considered here since there is no direct pathway for structure **1a** to fragment into the lowest energy structures of corresponding fragmented units.

To further estimate the energy required to break the central H–H bond in structure **1a**, we have scanned the potential energy surface at various H···H distances (the first fragmentation pathway) both at B3LYP and CCSD(T) levels, and the results are depicted in Fig. 2. At each point on the potential energy surface, the entire cluster was completely optimized with a fixed H–H distance at the B3LYP level. Furthermore, IR spectra for isomer **1a** reveal an IR active H–H unscaled stretching frequency at 1879 cm^{-1} , which strongly complements the existence of an elongated H–H bond. All these methods reflect significant energy barriers to break the H–H bond. This further confirms that the anion is kinetically stable toward dissociation along the selected pathway.

The nature of chemical bonding in isomer **1a** is studied by analyzing how the total number of electrons is distributed and the nature of frontier molecular orbitals. The total number of valence electrons in $\text{Al}_4\text{H}_{14}^-$ is 27, 3 from each Al atom [3×4 (Al)] and 1 from each H atom [1×12 (H)] plus the negative charge. How were these 27 electrons distributed? To understand that, we recall that there are two major types of bonds in aluminum hydrides, namely, $2c-2e$ Al–H_t terminal bonds and $3c-2e$ Al–H_b–Al bridge bonds. In the most stable structure, **1a**, there are nine Al–H_t terminal bonds, which account for 9×2 (18) electrons and six electrons from three Al–H–Al bonds counting to 24 electrons (18 + 6). This leaves three electrons, which should be distributed, between Al–H–H–Al atoms. Although it is tempting to associate two electrons to the bonding

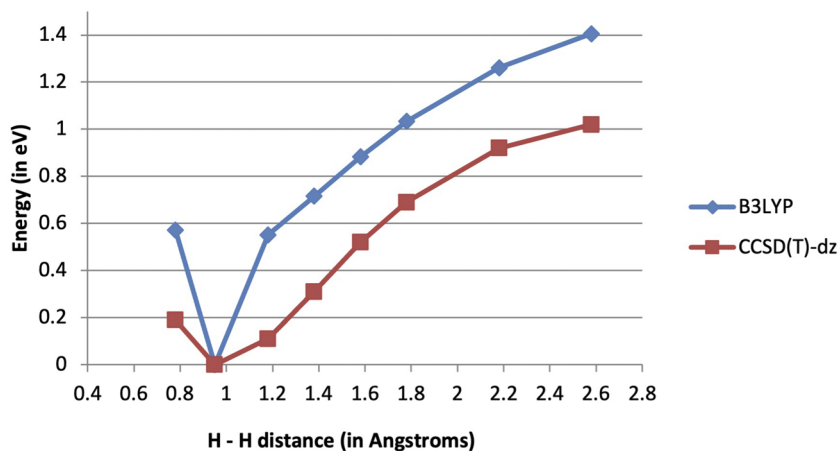


FIG. 2. The potential energy scan of structure **1a** at different H–H distances, calculated at B3LYP and CCSD(T) levels using the CC-pVDZ basis set. For each fixed H–H distance, the remaining part of the cluster was optimized at the B3LYP level.

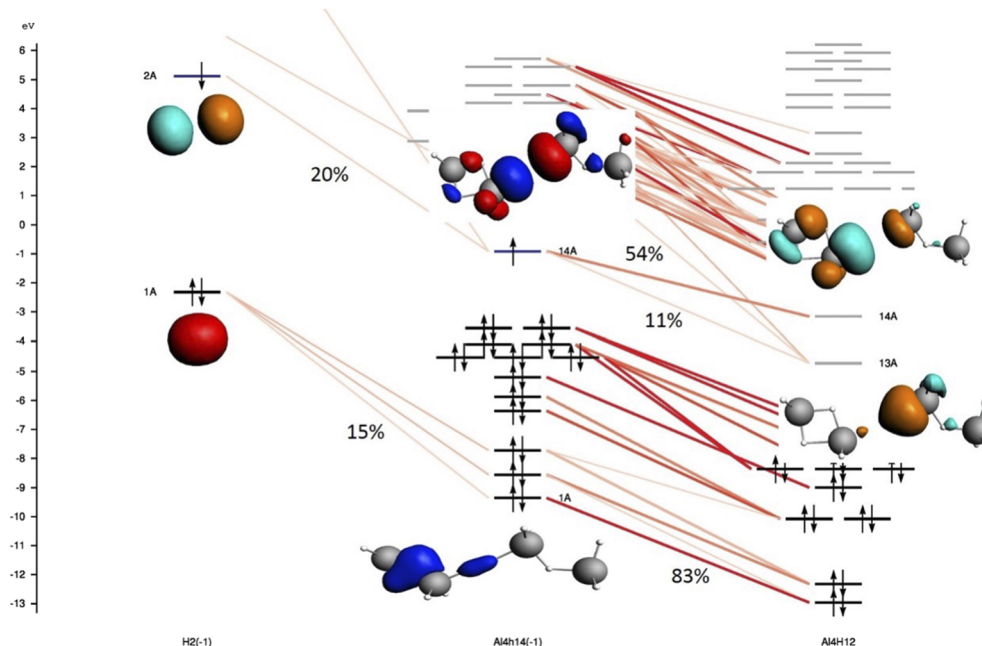


FIG. 3. Fragment Molecular Orbital (FMO) analyses of $\text{Al}_4\text{H}_{14}^-$ as calculated from ADF software. The geometry of $\text{Al}_4\text{H}_{14}^-$ was optimized at B3-LYP/cc-pVTZ and the FMO analysis done at the PW91/TZV2P level of theory. The MO energies are in eV. The red lines indicate the interactions (given in %) between H_2^- (left panel) and Al_4H_{12} (right panel). The corresponding MOs of the fragments and the complex are also shown.

and one electron to the antibonding between Al–H–Al atoms, it is an oversimplification. To get a clear picture of how H_2 interacts with aluminum atoms, we have carried out the Fragment Molecular Orbital (FMO) analysis¹⁵ on structure **1a**. The FMO calculations are done at the PW91/TZVP level, by utilizing the isomer (structure **1a**, here) optimized at B3LYP/cc-pVTZ, using the ADF suite of program.^{16–18} Structure **1a** can be viewed as H_2 is sandwiched between two Al_2H_6 units. The interaction diagram between H_2^- and Al_4H_{12} is given in Fig. 3. This diagram depicts the fragment contributions to each MO of $\text{Al}_4\text{H}_{14}^-$ (central panel) from H_2^- (left panel) and Al_4H_{12} (right panel). These contributions depend on the symmetry as well as the energy separation between the fragment MOs. As can be seen from the diagram, the major interactions between H_2^- and Al_4H_{12} are as follows. The sigma bonding orbital of H_2 strongly interacts with the low-lying Al_4H_{12} orbitals, giving rise to lowest MOs (1A–3A) of $\text{Al}_4\text{H}_{14}^-$. Pictures of these MOs (Fig. 3) show that these interactions are mainly driven by symmetry considerations rather than a strong overlap between Al atoms with H_2 . However, there is a minor bonding interaction (6%) between H_2 (1A) and Al_4H_{12} (13A), which contributes to the Al–H–Al bonding. The second major interaction is between H_2 sigma* (2A) with 14A of Al_4H_{12} to form SOMO of $\text{Al}_4\text{H}_{14}^-$. This single interaction provides the bulk of the bonding between H_2 with the two Al_2H_6 units. This is as if the two Al_2H_6 units are trapping H_2^- . If this is true, then removing that one electron should make the units fall apart. This is indeed true. Optimization of the neutral Al_4H_{14} dissociates the molecule into three units: two Al_2H_6 and H_2 . There is not even a stationary point on the potential energy surface holding all these units together. Note that both Al_2H_6 and H_2 are very stable molecules and

all these stable units are held together by *one single electron*. This unusual bonding has not been observed in any other hydrides.

In this Communication, we report a unique structure of $\text{Al}_4\text{H}_{14}^-$, wherein an H_2^- unit is trapped between two Al_2H_6 units, contributing toward the high intense peak of $\text{Al}_4\text{H}_{14}^-$ in the mass spectrum⁷ of aluminum hydrides. To our knowledge, this is the first time a molecular trap using aluminum hydride clusters to stabilize H_2^- is reported, thus further extending our knowledge of aluminum hydride clusters. The electron counting and fragment molecular orbital analysis have revealed a unique bonding pattern in this *bound* structure (isomer **1a**) of $\text{Al}_4\text{H}_{14}^-$, in which a *single electron* holds the three units, H_2^- and two Al_2H_6 units, together.

Part of this work was supported by the Air Force Office of Scientific Research (AFOSR) under Grant No. FA9550-19-1-0077 (K.H.B.). B. K. dedicates this article to Prof. E. D. Jemmis on the occasion of his 70th birthday.

DATA AVAILABILITY

The data that support the findings of this study are available from the corresponding authors upon reasonable request.

REFERENCES

- 1 R. Gosler, H. Gnaser, W. Kutschera, A. Priller, P. Steier, A. Wallner, and M. Cizek, *Phys. Rev. Lett.* **94**, 223003 (2005).
- 2 V. Rudnev, M. Schlösser, H. H. Telle, and Á. González Ureña, *Chem. Phys. Lett.* **639**, 41–46 (2015).
- 3 A. Grubisic, X. Li, S. T. Stokes, J. Cordes, G. F. Ganteför, K. H. Bowen, B. Kiran, P. Jena, R. Burgert, and H. Schnöckel, *J. Am. Chem. Soc.* **129**, 5969 (2007).

- ⁴B. Kiran, P. Jena, X. Li, A. Grubisic, S. T. Stokes, G. F. Ganteför, K. H. Bowen, R. Burgert, and H. Schnöckel, *Phys. Rev. Lett.* **98**, 256802 (2007).
- ⁵X. Li, A. Grubisic, S. T. Stokes, J. Cordes, G. F. Ganteför, K. H. Bowen, B. Kiran, M. Willis, P. Jena, R. Burgert, and H. Schnöckel, *Science* **315**, 356 (2007).
- ⁶B. Kiran, A. K. Kandalam, J. Xu, Y. H. Ding, M. Sierka, K. H. Bowen, and H. Schnöckel, *J. Chem. Phys.* **137**, 134303 (2012).
- ⁷X. Li, A. Grubisic, K. H. Bowen, A. K. Kandalam, B. Kiran, G. F. Ganteför, and P. Jena, *J. Chem. Phys.* **132**, 241103 (2010).
- ⁸D. M. Deaven and K. M. Ho, *Phys. Rev. Lett.* **75**, 288 (1995); M. Sierka, *Prog. Surf. Sci.* **85**, 398 (2010).
- ⁹TURBOMOLE V6.3 2011—A development of the University of Karlsruhe and Forschungszentrum Karlsruhe GmbH, 1987–2007, TURBOMOLE GmbH, since 2007; available from www.turbomole.com.
- ¹⁰M. J. Frisch, G. W. Trucks, H. B. Schlegel *et al.*, GAUSSIAN 09, Revision B.01, Gaussian, Inc., Wallingford, CT, 2004.
- ¹¹A. D. Becke, *J. Chem. Phys.* **98**, 5648 (1993).
- ¹²C. Lee, W. Yang, and R. G. Parr, *Phys. Rev. B* **37**, 785 (1988).
- ¹³J. Moc, *J. Mol. Model.* **18**, 3427–3438 (2012).
- ¹⁴M. Sobczyk, I. Anusiewicz, and P. Skurski, *J. Chem. Phys.* **118**(16), 7297 (2003).
- ¹⁵F. M. Bickelhaupt and E. J. Baerends, in *Reviews in Computational Chemistry*, edited by K. B. Lipkowitz and D. B. Boyd (Wiley, New York, 2000), Vol. 15, pp. 1–86.
- ¹⁶G. te Velde, F. M. Bickelhaupt, E. J. Baerends, C. Fonseca Guerra, S. J. A. van Gisbergen, J. G. Snijders, and T. Ziegler, “Chemistry with ADF,” *J. Comput. Chem.* **22**, 931 (2001).
- ¹⁷C. Fonseca Guerra, J. G. Snijders, G. te Velde, and E. J. Baerends, “Towards an order-N DFT method,” *Theor. Chem. Acc.* **99**, 391 (1998).
- ¹⁸SCM, Theoretical Chemistry, ADF2013, Vrije Universiteit, Amsterdam, The Netherlands, 2013. See <http://www.scm.com>.